Langmuir
Article
pubs.acs.org/Langmuir

Glucose Biosensor Based on Nanocomposite Films of CdTe Quantum Dots and Glucose Oxidase

Xinyu Li,[†] Yunlong Zhou,[‡] Zhaozhu Zheng,[†] Xiuli Yue,[§] Zhifei Dai,[†] Shaoqin Liu,*[,†,∥] and Zhiyong Tang[‡,*]

[†]*Nanomedicine and Biosensor Laboratory, Bio-X Center, Harbin Institute of Technology, Harbin 150080, China,* [‡]*National Center of Nanoscience and Technology, Beijing 100190, China,* [§]*School of Municipal and Environmental Engineering, Harbin Institute of Technology, Harbin 150001, China and* [∥]*Center for Micro and Nanotechnology, Harbin Institute of Technology, Harbin 150080, China*

Received January 7, 2009. Revised Manuscript Received February 5, 2009

A blood glucose sensor has been developed based on the multilayer films of CdTe semiconductor quantum dots (QDs) and glucose oxidase (GOD) by using the layer-by-layer assembly technique. When the composite films were contacted with glucose solution, the photoluminescence of QDs in the films was quickly quenched because the enzyme-catalyzed reaction product (H_2O_2) of GOD and glucose gave rise to the formation of surface defects on QDs. The quenching rate was a function of the concentration of glucose. The linear range and sensitivity for glucose determination could be adjusted by controlling the layers of QDs and GOD. The biosensor was used to successfully determine the concentration of blood glucose in real serum samples without sample pretreatment and exhibited satisfactory reproducibility and accuracy.

Introduction

Semiconductor quantum dots (QDs) have great application potential in the field of biosensors due to their excellent optical property and large specific surface area, which is easily accessible to the analytes.[1−5] However, QDs, themselves, do not have specific recognition toward the detected objects. Therefore, different types of biomolecules, including protein, enzyme, and DNA, are conjugated with QDs to form nanocomposites either in solution or on the substrate surface in order to offer selectivity of biosensors.[6−15] Although numerous physical or chemical strategies have been successfully applied to develop new nanocomposite biosensors, several disadvantages, for example, time and cost consumption, difficulty of large-scale production, and absence of universality, limit the practical applications of these methods. The electrostatic layer-by-layer (LBL) self-assembly technique introduced by Decher,[16] which is based on the alternative deposition of opposite-charged species on the substrates, may provide an alternative way to develop new generation of nanocomposite biosensors.[17−24] The simplicity, economy, universality, and friendly environment of film fabrication by LBL have contributed to the widespread popularity of this method.[25−29] Our previous studies on the LBL multilayers have demonstrated that the optical, electrical, and electrochemical response of nanoparticles in the multilayer film can be tailored through the layer architecture.[30,31] In the present investigation, such studies are extended to the biosensor field that the photoluminescent QDs and biospecific glucose oxidase (GOD) are integrated into the composite film by LBL

*To whom correspondence should be addressed. E-mail: shaoqinliu@hit.edu.cn (S.L.); zytang@nanoctr.cn (Z.T.).

(1) Brus, L. *Appl. Phys. A: Mater. Sci. Process.* **1991**, *53*, 465–474.
(2) Alivisatos, A. P. *Science* **1996**, *271*, 933–937.
(3) Nirmal, M.; Brus, L. *Acc. Chem. Res.* **1999**, *32*, 407–414.
(4) Grieve, K.; Mulvaney, P.; Grieser, F. *Curr. Opin. Colloid Interface Sci.* **2000**, *5*, 168–172.
(5) Costa-Fernández, J. M.; Pereiro, R.; Sanz-Medel, A. *Trends Anal. Chem.* **2006**, *25*, 207–218.
(6) Chan, W. C.; Maxwell, D. J.; Gao, X.; Bailey, R. E.; Han, M.; Nie, S. *Curr. Opin. Biotechnol.* **2002**, *13*, 40–46.
(7) Gill, R.; Zayats, M.; Willner, I. *Angew. Chem., Int. Ed.* **2008**, *47*, 7602–7625.
(8) Baron, R.; Willner, B.; Willner, I. *Chem. Commun.* **2007**, 323–332.
(9) Willner, I.; Basnar, B.; Willner, B. *FEBS J.* **2007**, *274*, 302–309.
(10) Somers, R. C.; Bawendi, M. G.; Nocera, D. G. *Chem. Soc. Rev.* **2007**, *36*, 579–591.
(11) Lee, J.; Hernandez, P.; Lee, J.; Govorov, A. O.; Kotov, N. A. *Nat. Mater.* **2007**, *6*, 291–295.
(12) Medintz, I. L.; Uyeda, H. T.; Goldman, E. R.; Mattoussi, H. *Nat. Mater.* **2005**, *4*, 435–446.
(13) Michalet, X.; Pinaud, F. F.; Bentolila, L. A.; Tsay, J. M.; Doose, S.; Li, J. J.; Sundaresan, G.; Wu, A. M.; Gambhir, S. S.; Weiss, S. *Science* **2005**, *307*, 538–544.
(14) Rosi, N. L.; Mirkin, C. A. *Chem. Rev.* **2005**, *105*, 1547–1562.
(15) Mitchell, G. P.; Mirkin, C. A.; Letsinger, R. L. *J. Am. Chem. Soc.* **1999**, *121*, 8122–8123.
(16) Decher, G. *Science* **1997**, *277*, 1232–1237.
(17) Tang, Z.; Wang, Y.; Podsiadlo, P.; Kotov, N. A. *Adv. Mater.* **2006**, *18*, 3203–3224.
(18) Jiang, C.; Tsukruk, V. V. *Adv. Mater.* **2006**, *18*, 829–840.
(19) Constantine, C. A.; Gattás-Asfura, K. M.; Mello, S. V.; Crespo, G.; Rastogi, V.; Cheng, T. C.; DeFrank, J. J.; Leblanc, R. M. *Langmuir* **2003**, *19*, 9863–9867.
(20) Zhang, X.; Chen, H.; Zhang, H. Y. *Chem. Commun.* **2007**, 1395–1405.
(21) Zhang, X.; Sun, Y. P.; Shen, J. C. In *Protein Architecture: Interfacing molecular assemblies and immobilization biotechnology*; Lvov, Y., Möhwald, H., Eds.; Marcel Dekker, Inc.: New York, **2000**; Chapter 9, pp 229−249.
(22) Lisdat, F.; Dronov, R.; Möhwald, H.; Scheller, F. W.; Kurth, D. G. *Chem. Commun.* **2009**, 274–283.
(23) Dronov, R.; Kurth, D. G.; Möhwald, H.; Scheller, F. W.; Lisdat, F. *Angew. Chem., Int. Ed.* **2008**, *47*, 3000–3003.
(24) Dronov, R.; Kurth, D. G.; Möhwald, H.; Spricigo, R.; Leimkühler, S.; Wollenberger, U.; Rajagopalan, K. V.; Scheller, F. W.; Lisdat, F. *J. Am. Chem. Soc.* **2008**, *130*, 1122–1123.
(25) Hammond, P. T. *Curr. Opin. Colloid Interface Sci.* **2000**, *4*, 430–442.
(26) Decher, G.; Eckle, M.; Schmitt, J.; Struth, B. *Curr. Opin. Colloid Interface Sci.* **1998**, *3*, 32–39.
(27) Knoll, W. *Curr. Opin. Colloid Interface Sci.* **1996**, *1*, 137–143.
(28) Yu, A.; Liang, Z.; Caruso, F. *Chem. Mater.* **2005**, *17*, 171–175.
(29) Podsiadlo, P.; Kaushik, A. K.; Arruda, E. M.; Waas, A. M.; Shim, B. S.; Xu, J.; Nandivada, H.; Pumplin, B. G.; Lahann, J.; Ramamoorthy, A.; Kotov, N. A. *Science* **2007**, *318*, 80–83.
(30) Liu, S.; Kurth, D. G.; Volkmer, D. *Chem. Commun.* **2002**, 976–977.
(31) Wang, Y.; Tang, Z.; Correa-Duarte, M. A.; Liz-Marzán, L. M.; A., K. N. *J. Am. Chem. Soc.* **2003**, *125*, 2830–2831.

techniques, and the nanocomposite exhibits good optical response toward glucose.

The measurement of glucose concentration in blood is critical for diagnosis of diabetes mellitus, which is affecting about 150 million people in the world.[32] Millions of diabetics need to test their blood glucose levels daily, making glucose the most commonly tested analyte. Since Clark and Lyons proposed in 1962 the initial concept of glucose enzyme electrodes,[33] many impressive advances in the design and use of glucose biosensors have been achieved, and actually glucose biosensors account for about 85% of the entire biosensor market.[34,35] Among those, the conjugates of QDs and GOD in solution have also been explored as highly sensitive glucose biosensors.[36−38]

Herein, we sought to develop a glucose sensor using the immoblized QD/GOD multilayer film on an optically transparent substrate by LBL techniques. In addition to easy storage and transport, our choice of a surface, rather than a solution-based sensor, is based on possible realization of the chip-based sensors, which are designed in an array format for rapid, high-throughput detection. Moreover, previous reports have confirmed that, by rational design, the multilayer films showed controlled permeability toward different types of ions and molecules,[39−43] a property required for separation and sensing technologies. Therefore, it can be anticipated that the LBL-based combination of QDs as photoluminence probes and GOD as biocatalyst shows great promise as optical sensors for glucose with tailored catalytic properties and permselectivities.

Experimental Section

Materials and Methods. $Cd(ClO_4)_2 \cdot 6H_2O$, Al_2Te_3 powders, and mercaptopropionic acid (MPA) were purchased from Alfa Aesar. Glucose oxidase (GOD, EC 1.1.3.4 from *Aspergillus niger*, lyophilized, 151 U mg^{-1} solid), glucose, sodium polystyrenesulfonate (PSS, MW 70 000), and poly(allylamine hydrochloride) (PAH, MW 8000−11000) were purchased from Sigma-Aldrich. Enzyme working solutions were prepared by dissolving the lyophilizate in phosphate buffer solution (pH 7.4, 20 mM). Other reagents were commercially available and were of analytical reagent grade. All solutions were prepared with ultrapure water from a Milli-Q water purification system (Billerica, MA).

The UV−vis absorption spectra were measured by using a Varian Cary 4000 UV−vis spectrometer (Varian, Inc.), and the photoluminescence spectra were recorded with a Cary Eclipse fluorescence spectrophotometer (Varian, Inc.). If not specially stated, the samples were excited at 380 nm, and the exciting slit and the emission slit were 5 and 10 nm, respectively. The optical properties of solutions and the multilayer films were measured using quartz cuvettes of 10 mm path length and a standard solid sample holder, respectively.

Synthesis of MPA-Modified CdTe QDs. A total of 0.986 g of $Cd(ClO_4)_2 \cdot 6H_2O$ was dissolved in 125 mL of distilled water, and then 0.43 mL of MPA was added. The pH value was adjusted to 11.2 by adding 2 M NaOH. The solution was placed in a three-neck flask and deaerated by N_2 gas for about 30 min. H_2Te gas generated by the mixture of 0.2 g of Al_2Te_3 and 15 mL of 0.5 M H_2SO_4 in another three-neck flask was directed into the prepared solution. CdTe QDs with photoluminescence peaks at 612 nm were obtained by refluxing the solution for 48 h in nitrogen gas. The QD solution could maintain its optical characteristics for at least 1 year when placed in a refrigerator at 4 °C.

Layer-by-Layer Assembly of $(PAH/CdTe)_x(PAH/PSS)_3(PAH/GOD)_y$ Multilayer. Quartz or glass substrates were cleaned according to literature procedures.[44−46] Previous studies showed that the permeability of the polyelectrolyte multilayers toward redox-active ions and molecules, a property required for separation and sensing technologies, was controlled;[39−43] therefore, the ionic strength of the solutions was adjusted with NaCl as mentioned in the text. Scheme 1 presents an overview of the procedure used for the film assembly.

First, CdTe QDs/PAH multilayers were prepared by alternatively depositing PAH and CdTe QDs onto the substrates. These QD/PAH multilayers were alternatively deposited from 1 mg/mL PAH aqueous solutions (pH 7.4, 0.5 M NaCl) and the prepared QD solution, using an immersion time of 10 min, followed by rinsing with water and drying under N_2 flow after each layer deposition. For each cycle, a bilayer of PAH/QDs was formed, and the UV−vis and photoluminescence spectra of the growing layers were recorded in air after each assembly cycle. This cycle procedure was repeated many times until a stable film was obtained. On top of this stable bilayer system, three bilayers of PAH/PSS were deposited by alternative immersion in 1 mg/mL PAH and PSS aqueous solution (pH 7.4, 0.5 M NaCl) each for 10 min. Three bilayers of PAH/PSS were used for avoiding possible interference of glucose or other species in samples. Finally, deposition of the capping layers of PAH/GOD yielded the multilayers of $(PAH/CdTe)_x(PAH/PSS)_3(PAH/GOD)_y$. The pH of phosphate-buffered saline (PBS) solution containing GOD was 7.4. The isoelectric point of GOD is 4.2, so at pH 7.4 the enzyme was negatively charged. Moreover, in order to enhance the permeability to glucose, a PAH solution without NaCl and 0.5 mg/mL GOD PBS solution (20 mM) were used for the fabrication of the capping layers. The multilayer system of CdTe QDs, GOD, and PEs was referred as the sensing assembly and was used for the detection of glucose.

Glucose Calibration. In a thermostatted titration, 3 mL of PBS solution was pipetted into fluorescence quartz cuvettes. This solution was left to equilibrate at 37 °C, and the glass slides modified with the sensing assembly for the photoluminescence measurements were dipped into the stirred cuvettes. The kinetic measurements of photoluminescence at 630 nm were then run in the absence of glucose substrate for 1−5 min, and subsequently the glucose stock solutions of different volumes were injected in the cuvettes. The decrease of the photoluminescence intensity at 630 nm was recorded with time for 100 min. Several sets of samples containing different concentrations of glucose were prepared by diluting the stock solution (0.5 M) into 3 mL of PBS. The relationship between decrease rates of photoluminescence and the glucose concentration was plotted for the standard curve, which was used in detection of glucose in the real serum samples.

Glucose Detection in Real Serum Samples. To avoid possible interference from fluorescent reagents such as protein, the procedure for glucose determination in serum samples was as follows: As a reference experiment, the glass slide modified with

(32) Wilson, J. F. *Ann. Intern. Med.* **2007**, *146*, ITC1-15.
(33) Clark, L. C.; Lyons, C. *Ann. N.Y. Acad. Sci.* **1962**, *102*, 29–45.
(34) Wang, J. *Chem. Rev.* **2008**, *108*, 814–825.
(35) Heller, A.; Feldman, B. *Chem. Rev.* **2008**, *108*, 2482–2505.
(36) Gill, R.; Bahshi, L.; Freeman, R.; Willner, I. *Angew. Chem., Int. Ed.* **2008**, *47*, 1676–1679.
(37) Yuan, J.; Guo, W.; Wang, E. *Anal. Chem.* **2008**, *80*, 1141–1145.
(38) Huang, C.-P.; Liu, S.-W.; Chen, T.-M.; Li, Y.-K. *Sens. Actuators, B* **2008**, *130*, 338–342.
(39) Harris, J. J.; Bruening, M. L. *Langmuir* **2000**, *16*, 2006–2013.
(40) Dai, J.; Jensen, A. W.; Mohanty, D. K.; Eradt, J.; Bruening, M. L. *Langmuir* **2001**, *17*, 931–937.
(41) Farhat, T. R.; Schlenoff, J. B. *Langmuir* **2001**, *17*, 1184–1192.
(42) Liu, S.; Kurth, D. G.; Bredenkotter, B.; Volkmer, D. *J. Am. Chem. Soc.* **2002**, *124*, 12279–12287.
(43) Liu, S.; Volkmer, D.; Kurth, D. G. *Anal. Chem.* **2004**, *76*, 4579–4582.
(44) Kern, W. *RCA Eng.* **1983**, *28*, 99–105.
(45) Philips, B. F. *J. Vac. Sci. Technol., A* **1983**, *A1*, 646.
(46) Kern, W. *Semicond. Int.* **1984**, 94–99.

Scheme 1. Sensing Assembly: (a) Top 3 Bilayers of PAH/GOD, (b) 3 Bilayers of PAH/PSS, and (c) 12 Bilayers of PAH/CdTe QDs

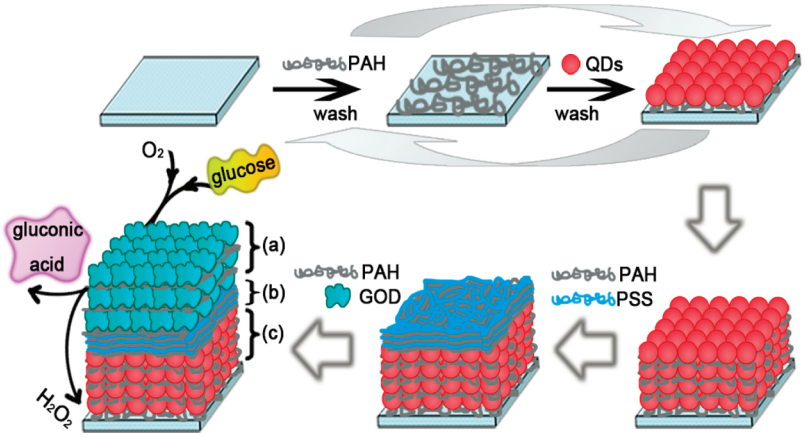

the sensing assembly was first dipped in the blank PBS solution, and the emission spectrum of the sensing assembly was taken. The sensing assembly was then dried under N_2 flow and incubated with the serum sample at 37 °C for a fixed time interval of 5 min. After being rinsed with PBS and dried under N_2 flow, the emission spectrum of the sensing assembly was measured again in PBS solution. The difference between photoluminescence intensities at 630 nm before and after immersion into serum samples was compared with the standard curve, and then the glucose concentration in the serum sample was obtained.

Results and Discussion

Rational Design of Nanocomposite Films as Glucose Biosensors. The organized integration of CdTe QDs with high photoluminescence and GOD with specific recognition may allow us to prepare glucose biosensors with high sensitivity. The biosensing mechanism is outlined as follows: First, GOD catalytically oxidizes glucose to gluconolactone, and meanwhile the FAD groups in GOD enzymes are reduced to $FADH_2$ (eq 1). Subsequently, the $FADH_2$ groups in GOD are easily oxidized by O_2 in solution to produce H_2O_2 (eq 2). Finally, H_2O_2 chemically etches the QDs to generate many surface defects, leading to quenching of QD photoluminescence (eq 3).[36] By monitoring the photoluminescence change, one can calculate the glucose concentration in the samples.

$$\text{glucose} + \text{FAD} - \text{GOD} \rightarrow \text{gluconolactone} + \text{FADH}_2\text{–GOD} \quad (1)$$

$$\text{FADH}_2\text{–GOD} + \text{O}_2 + \text{H}_2\text{O} \rightarrow \text{FAD} - \text{GOD} + \text{H}_2\text{O}_2 \quad (2)$$

$$\text{H}_2\text{O}_2 + \text{QD (luminescent)} \rightarrow \text{H}_2\text{O} + \text{QD (nonluminescent)} \quad (3)$$

On the basis of the above biosensing principle, we design the layered hierarchical nanostructures composed of GOD and CdTe (Scheme 1). The outer layers of PAH/GOD are expected to contact and react with glucose in solution. The produced H_2O_2 further reacts with the CdTe QDs in the underlying multilayer of PAH/QD to result in quenching of their photoluminescence. Between PAH/GOD and PAH/QD multilayers, three bilayers of PAH/PSS are added in order to avoid possible influences of GOD−glucose reaction on the structures of underlying PAH/QD multilayers.

Spectroscopic Studies of the LBL Films of PAH/CdTe QDs. The multilayers of PAH/CdTe QDs were first deposited onto the glass substrates. Figure 1 represents the UV−vis absorption (black line) and photoluminescence (blue line) spectra of MPA-capped CdTe QDs in solution. The absorbance shoulder of QDs is located at 560 nm, while the photoluminescence peak of QDs is situated at 612 nm. The size and concentration of CdTe QDs in solution are estimated from the UV−vis spectrum to be around 3.4 nm and 5.58×10^{-5} mol L^{-1}, respectively, according to the formula in Peng's paper.[47] The stabilizers of CdTe QDs, mercaptopropionic acid (MPA), offer negative surface charges due to deprotonation of the carboxylic acid end groups in base solution. Therefore, PAH/CdTe QDs multilayers can be prepared by alternatively depositing positively charged PAH and negatively charged CdTe QDs onto the negatively charged substrates such as glass, quartz, or silica.

The LBL assembly process of PAH and QDs was monitored by the absorbance increase in UV−vis absorption spectroscopy. Figure 2 shows the UV−vis spectra of $(PAH/CdTe\ QDs)_x$ multilayers deposited on a glass substrate, where the first layer is PAH and the outermost layer is QDs. The absorbance shoulder at 567 nm (λ_{567nm}) increases steadily with the number of bilayers, x, which confirms irreversible adsorption of PAH and QDs on the substrate. The inset shows a plot of λ_{567nm} versus the number of bilayers. Regular layer growth is revealed by a linear dependence of the absorbance determined at 567 nm versus x, and the absorbance increase for one bilayer of PAH/CdTe QDs at 567 nm is 0.0052 ± 0.0003. It is also noted that there is deviation from linear behavior for a small number of bilayers, which can be explained by incomplete coverage of QDs and partial filling of the polyelectrolyte into the empty space between QDs during the early stage of LBL deposition. This phenomenon has already been reported for nanoparticle/polyelectrolyte LBL multilayers by other groups. [48]

PAH/CdTe QD Multilayer Exposed to H_2O_2. In order to determine the response of multilayers toward H_2O_2, we examined the photoluminence change of the immobilized PAH/CdTe QDs multilayer exposed to H_2O_2 solution.

(47) Yu, W. W.; Qu, L.; Guo, W.; Peng, X. *Chem. Mater.* **2003**, *15*, 2854–2860.
(48) Jiang, C. Y.; Markutsya, S.; Tsukruk, V. V. *Langmuir* **2004**, *20*, 882–890.

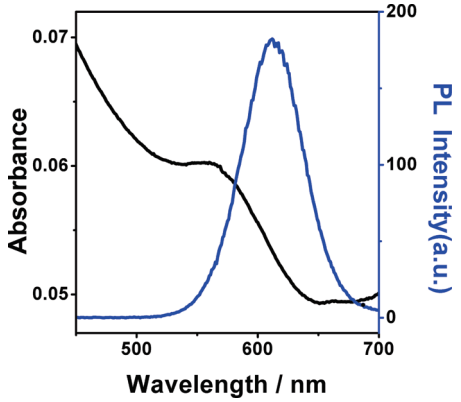

Figure 1. UV−vis (black line) and luminescence spectra (blue line) of MPA-capped CdTe QDs in solution.

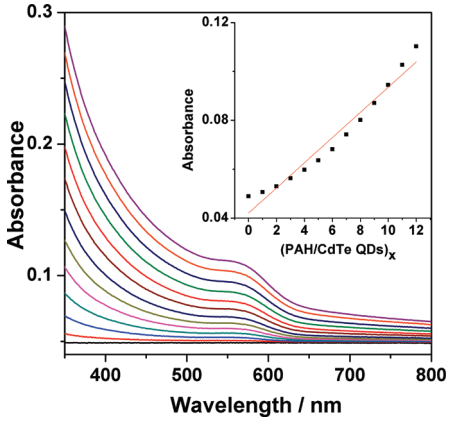

Figure 2. UV−vis spectra of growing PAH/CdTe QD multilayers (1−12). Inset shows a plot of λ_{567nm} versus the number of bilayers, x.

Figure 3A shows the spectra of 12 bilayers of PAH/MPA-capped CdTe QDs before and after incubation with 0.2 mM H_2O_2 solution at 37 °C. Before incubation, the PAH/CdTe QDs multilayer has a strong photoluminescence peak at 630 nm, which exhibits a red shift of 18 nm in the peak wavelength compared with that of QDs in solution. The red shift of the photoluminescence peak should be ascribed to the Förster resonance energy transfer between the closely adjacent QDs in the multilayer film, which was also observed in the previous report.[49−52] When 0.2 mM H_2O_2 is added into the PBS solution, a significant decrease in the photolumimenscne peak at 630 nm is instantly observed (as shown in curve b in Figure 3A). Such photoluminescence quenching originates from the production of surface defects on QDs by H_2O_2, which can prevent radiative recombination of electrons and holes by trapping these carriers.[53−56] The photoluminescence change at 630 nm is further monitored

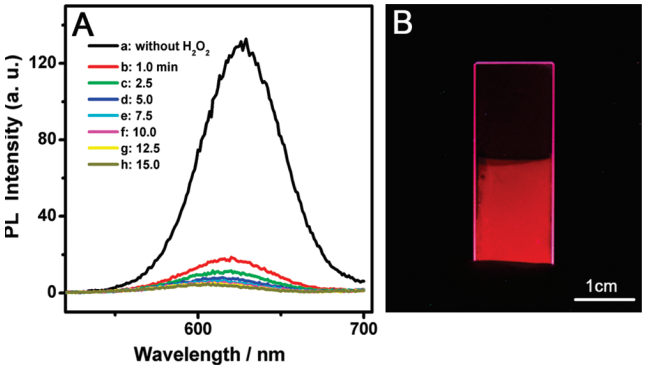

Figure 3. (A) Time-dependent photoluminescence changes upon the interaction of 12 bilayers of PAH/CdTe QDs in the absence (a) and presence (b−h) of 0.2 mM H_2O_2. All measurements were performed in a 20 mM phosphate buffer solution, pH = 7.4. The samples were excited at 380 nm, and the exciting slit and the emission slit were 5 nm. (B) UV photograph of 12 bilayers of PAH/CdTe QDs after H_2O_2 exposure for 1 min. The upper part of the slide exposed in 0.2 mM H_2O_2 solution is bleached, while the lower part has no obvious photoluminescence change.

in a real time, and its intensity decreases as time increases (Figure 3A, curves c−h). The quenching is easily visualized by the naked eye. Figure 3B illustrates UV photographs of 12 bilayers of PAH/CdTe QDs after H_2O_2 exposure. After half of the coated glass was incubated with 0.2 mM H_2O_2 solution for 1 min, one can see that the photoluminescence of the part exposed to H_2O_2 is totally quenched while the photoluminescence of the unexposed part remains unchanged. Moreover, the decrease rate of the photoluminescence intensity of PAH/CdTe QD multilayers is dependent on H_2O_2 concentration in solution (not shown). This property results in direct determination of the concentration of the analytes, which can produce H_2O_2, by measuring the decrease rate of photoluminescence intensity (see below).

Spectroscopic Studies of the $(PAH/CdTe)_x(PAH/PSS)_3(PAH/GOD)_y$ Multilayer. As discussed above, $(PAH/CdTe)_x(PAH/PSS)_3(PAH/GOD)_y$ multilayer films were prepared, and the experimental conditions were optimized for direct determination of the concentration of the glucose.

Because the reduction product of GOD, the acid anion (gluconolactone), may result in a decrease of the pH value of the electrolyte solution, 20 mM PBS buffer solution is used to maintain the pH value of the solution during the determination of glucose. First, the effect of reaction temperature on the decrease rate of the photoluminescence intensity of the multilayers at 630 nm is investigated ranging from 28 to 45 °C (Figure 4A). At different temperatures, the kinetic curves obtained for $(PAH/CdTe)_{12}(PAH/PSS)_3(PAH/GOD)_3$ in the presence of 4 mM glucose exhibit similar characteristics: After the addition of glucose, the photoluminescence intensity at 630 nm initially decreases linearly. When a certain period of time (ca. 10 min) has elapsed, gradually, the rate of decrease becomes smaller and finally achieves zero (Figure 4A). A larger rate of photoluminescence decrease is found at 37 °C (the inset in Figure 4A), and thus, the measurements for glucose calibration and glucose in a real serum sample are conducted at 37 °C. Further, the effect of pH value ranging from 6.0 to 9.0 on the decrease rate of the photoluminescence intensity at 630 nm is explored (not shown). At pH 9.0, the photoluminescence intensity of CdTe QDs is higher, but the bound enzyme loses most activity, resulting in the lower sensitivity. With the decrease

(49) Kagan, C. R.; Murray, C. B.; Nirmal, M.; Bawendi, M. G. *Phys. Rev. Lett.* **1996**, *76*, 1517–1520.
(50) Zucolotto, V.; Gattás-Asfura, K. M.; Tumolo, T.; Perinotto, A. C.; Antunes, P. A.; Constantino, C. J. L.; Baptista, M. S.; Leblanc, R. M.; Oliveira, O. N., Jr. *Appl. Surf. Sci.* **2005**, *246*, 397–402.
(51) Reinhard, B. M.; Siu, M.; Agarwal, H.; Alivisatos, A. P.; Liphardt, J. *Nano Lett.* **2005**, *5*, 2246–2252.
(52) Maier, S. A.; Kik, P. G.; Atwater, H. A. *Appl. Phys. Lett.* **2002**, *81*, 1714–1716.
(53) Woggon, U. *Optical Properties of Semiconductor Quantum Dots*; Springer: Berlin, **1997**; pp 159−177.
(54) Wang, Z.; Li, J.; Liu, B.; Hu, J.; Yao, X.; Li, J. *J. Phys. Chem. B* **2005**, *109*, 23304–23311.
(55) Burda, C.; Green, T. C.; Link, S.; El-Sayed, M. A. *J. Phys. Chem. B* **1999**, *103*, 1783–1788.
(56) Hagfeldt, A.; Grätzel, M. *Chem. Rev.* **1995**, *95*, 49–68.

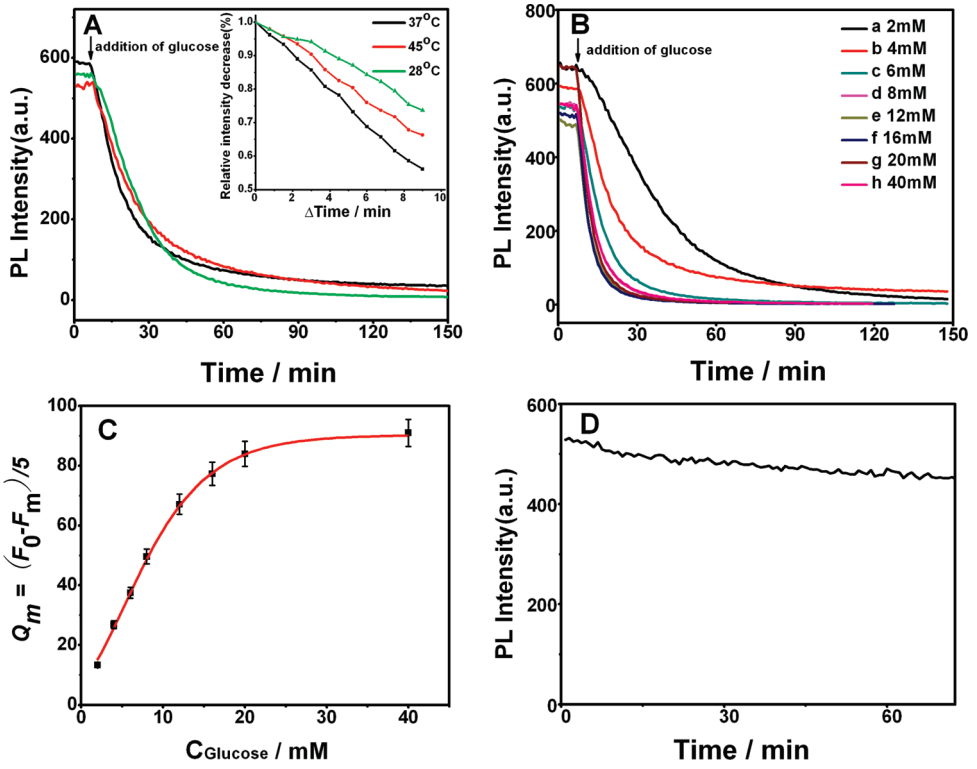

Figure 4. (A) Photoluminescence changes at 630 nm upon the interaction of $(PAH/CdTe)_{12}(PAH/PSS)_3(PAH/GOD)_3$ multilayer with 4 mM glucose solution at different temperatures. Inset presents the time-dependent photoluminescence change of multilayers during the first 9 min of reaction. (B) Time-dependent fluorescence changes recorded at 630 nm upon the interaction of $(PAH/CdTe)_{12}(PAH/PSS)_3(PAH/GOD)_3$ multilayer with variable concentrations of glucose: (a) 2, (b) 4, (c) 6, (d) 8, (e) 12, (f) 16, (g) 20, and (h) 40 mM. (C) Absolute quenching rate of the photoluminescence intensity taken from (B) within 5 min as a function of glucose concentration. F_0 and F_m represent the photoluminescence intensity of $(PAH/CdTe)_{12}(PAH/PSS)_3(PAH/GOD)_3$ multilayer at emission maximum in the absence (F_0) and presence (F_m) of glucose. (D) Time-dependent fluorescence changes recorded at 630 nm upon the interaction of $(PAH/CdTe)_{12}(PAH/PSS)_3$ multilayer with 2 mM glucose. All measurements were performed in a 20 mM phosphate buffer solution, pH = 7.4.

of solution pH, the photoluminescence intensity of CdTe QDs significantly decreases and becomes very small at pH 6.0. Finally, 7.4 is chosen as the optimal pH value of solution.

Figure 4B shows typical kinetic curves obtained for different glucose concentration levels at optimal conditions. The initial reaction rate for the first 5 min can be correlated with glucose concentration. Therefore, we use 5 min as the typical responding time in our study. The absolute photoluminescence intensity at 630 nm before (F_0) and the first 5 min (F_m) after the addition of glucose is taken, and then the absolute quenching rate of the sensing assembly, Q_m, can be calculated for the first 5 min after the initiation of enzyme reaction using the following equation:

$$Q_m = \frac{F_0 - F_m}{5} \quad (4)$$

Using the absolute quenching rate for the first 5 min after the initiation of enzyme reaction as a signal, we plot the quenching rate of the photoluminescence intensity for the first 5 min against glucose concentration, and the sensing assembly−glucose response curves are obtained (Figure 4C). The absolute quenching rates increase linearly with increasing glucose concentration until a substrate concentration of 16 mM is reached. The detection limit and the dynamic range for $(PAH/CdTe)_{12}(PAH/PSS)_3(PAH/GOD)_3$ is 0.5 mM and 0.5—16 mM, respectively. When the concentration of glucose is above this value, the curve levels off. In other words, a hyperbolic dependence is found for the $(PAH/CdTe)_{12}(PAH/PSS)_3(PAH/GOD)_3$ multilayer, which is in accordance

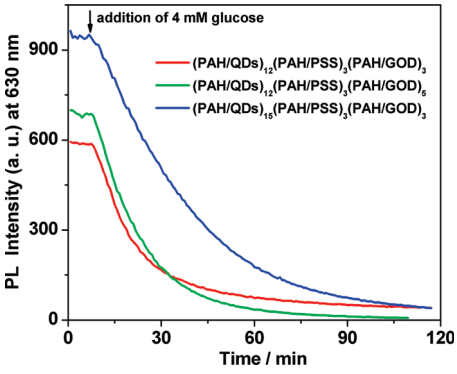

Figure 5. Time-dependent photoluminescence changes recorded at 630 nm upon the interaction of $(PAH/CdTe)_x(PAH/PSS)_3(PAH/GOD)_y$ multilayer with 4 mM glucose (λ_{exc} = 380 nm). All measurements were performed in a 20 mM phosphate buffer solution, pH = 7.4, thermostatted at 37 °C.

with the enzymatic kinetic study of GOD if we view the absolute quenching rate as the initial rate of enzyme reaction. On the basis of Michaelis−Menten theory,[57] the concentration of enzyme−substrate complex, which is proportional to the reaction rate, has a hyperbolic dependence on the initial concentration of substrate and remains constant during the reaction. The Y axis in Figure 4C indicates that the maximum quenching rate is ~90, which represents the maximum rate of catalytic reaction due to the saturation of active sites

(57) Cornish-Bowden, A. *Fundamentals of Enzyme Kinetics*; Butterworth: London, **1979**; pp 17−38.

Table 1. Determination of Blood Sugar in Real Serum Sample by Different Methods[a]

method	absolute quenching rate	corresponding concentration	average value
proposed method in this work	22.2	3.3	3.2 (pooled RSD = 10%)
	18.2	2.7	
	23.6	3.6	
	Beckman Coulter Unicel DxC600		3.1

[a] Each sample was analyzed by reacting the $(PAH/CdTe)_{12}(PAH/PSS)_3(PAH/GOD)_3$ multilayers with real serum sample for a fixed time interval of 5 min. All measurements were performed in a 20 mM phosphate buffer solution, pH = 7.4, thermostated at 37 °C.

on the enzyme. It is known that the Michaelis constant refers to the substrate concentration at which an enzyme reaction proceeds at half the maximum rate, which is 45 in our case. So, we obtain the Michaelis constant of three layers of GOD at ~8 mM, indicating that the enzyme has a higher affinity with the substrate.[58−60]

The contrast experiments, the photoluminescence spectra of PAH/CdTe QD multilayers in series of glucose and gluconolactone solutions, are also taken and show no significant change in the intensity of photoluminescence. On the basis of the fact that glucose only shows slight quenching effect on the PAH/CdTe QDs multilayers (from Figure 4D, the absolute quenching rate is only 0.5), one can see that incorporation of GOD layers in multilayer structures is necessary for the enzyme-catalyzed reaction to produce H_2O_2, which accounts for quenching of the photoluminescence intensity of QDs in the multilayer film. The above facts suggest that the quenching rate is directly proportional to the concentration of H_2O_2 produced from the enzyme-catalyzed reaction. In other words, the maximum reaction rate due to the binding of glucose or the formation of the enzyme−substrate complex is responsible for the highest detection limit of the sensing assembly. Therefore, the sensitivity and the linear range of the sensing assembly is attempted to be improved by controlling the layers' number of QDs and GOD. Different samples with various numbers of QDs and GOD layers are prepared, and kinetic curves for different samples with various numbers of QDs and GOD layers are obtained in the presence of 4 mM glucose (Figure 5). The quenching rate of the photoluminescence intensity within the initial 5 min is 26, 33, and 21 for $(PAH/CdTe)_{12}(PAH/PSS)_3(PAH/GOD)_3$, $(PAH/CdTe)_{12}(PAH/PSS)_3(PAH/GOD)_5$, and $(PAH/CdTe)_{15}(PAH/PSS)_3(PAH/GOD)_3$ multilayers, respectively. From the above data, we conclude the following: First, when the GOD layers are same, the quenching rates slightly decrease with the increase of QD layers (26 for 12 layers of QDs versus 21 for 15 layers of QDs). This tendency is due to the fact that the thinner multilayer of PAH/CdTe has better permeability toward H_2O_2. According to deviations from linear growth behavior observed for a small number of bilayers (Figure 2), one can know that during the early stage of LBL deposition, coverage of QDs is incomplete and the empty space between QDs is partially filled with the polyelectrolyte. As a result, the thinner multilayer of PAH/CdTe has more defects and is more permeable compared with thicker multilayer. Second, when the number of QD layers remains unchanged, the quenching rate of the photoluminescence intensity increases almost linearly with the layer number of enzyme (26 for 3 layers of GOD versus 33 for 5 layers of GOD). The increase of the quenching rate with the layer number of GOD may originate from the good permeability of the capping GOD multilayer toward glucose. In our experiment, a PAH solution without NaCl and 0.5 mg/mL GOD PBS solution (20 mM) were used for the fabrication of the capping layers. Our previous study[42] confirmed that small molecules could freely diffuse through the multilayer, which was prepared with salt-free PAH solution. This result demonstrates that the layer-by-layer immobilization process does not obviously affect the enzyme activity. The above results indicate that we can adjust the sensitivity and the linear range of the sensing assembly by controlling the layers of QDs and GOD.

When stocked at 4 °C, the sensing assembly can keep the same absolute quenching rate for detection of 2 mM glucose in the first week. The absolute quenching rate for detection of 2 mM glucose decreases by about 31% within 3 weeks after enzyme immobilization, although the fluorescence intensity of the sensing assembly remains unchanged. So, we conclude that the decrease of the absolute quenching rate results from the loss of enzyme activity. The sensing assembly is considered to be nonfunctional when its absolute quenching rate has fallen to about 70% of its original value. However, when stocked at −20 °C, our experimental results demonstrate that the sensing assembly can keep the same absolute quenching rate for detection of 2 mM glucose at least for 1 month.

Determination of Glucose in Real Serum Samples. The application of the present method in detection and determination of blood glucose in real serum samples has been investigated and compared with that measured by a hospital-used instrument (Beckman Coulter Unicel DxC600). Table 1 lists the measurement results. Evidently, the results obtained by our method are closer to that measured with the hospital-used instrument, and furthermore, the detection sensitivity of $(PAH/CdTe)_{12}(PAH/PSS)_3(PAH/GOD)_3$ multilayers also satisfies the diagnosis requirement of diabetes (the blood glucose concentration of healthy people is usually in the 4−8 mM range, while in patients with diabetes the range is much wider, 2−30 mM).

Conclusion

We present the design and implementation of a biosensor based on nanocomposite films of CdTe QDs and GOD for the detection and determination of glucose. The linear range and sensitivity of glucose determination can be adjusted by controlling structures of QDs and GOD in the sensing assembly. Blood glucose in real serum sample has been determined successfully using the proposed method with satisfactory reproducibility (as shown by RSD in Table 1) and accuracy without sample pretreatment. Although the sensor is for one-time use only because its fluorescence can partly recover (about only 30% of the original fluorescence intensity is recovered by keeping it overnight under ambient condition), the sensing assembly can be deposited on any size, any shape, and type of

(58) Liu, Y.; Feng, X.; Shen, J.; Zhu, J.-J.; Hou, W. *J. Phys. Chem. B* **2008**, *112*, 9237–9242.
(59) Wu, B.-Y.; Hou, S.-H.; Yin, F.; Li, J.; Zhao, Z.-X.; Huang, J.-D.; Chen, Q. *Biosens. Bioelectron.* **2007**, *22*, 838–844.
(60) Zhou, Q.; Xie, Q.; Fu, Y.; Su, Z.; Jia, X. e.; Yao, S. *J. Phys. Chem. B* **2007**, *111*, 11276–11284.

substrate in a cheap and automated way. Thus, it may be used as chip-based sensors,[61] which are designed in an array format for rapid, high-throughput screening of diabetes mellitus.

(61) Gao, J.; Liu, D.; Wang, Z. *Anal. Chem.* **2008**, *80*, 8822–8827.

Acknowledgment. The authors thank the National High-Tech Research and Development Program (2007AA03Z302, Z.Y.T., S.Q.L., X.Y.L.), 100-talent program of Chinese Academy of Sciences (Z.Y.T.), and start-up funding of HIT (S.Q.L.) for financial support of this research.